

# Molecular Reorganizations of Rod–Coil Molecules on a Solid Surface

Vladimir V. Tsukruk,<sup>\*,†</sup> Kirsten Genson,<sup>†</sup> Sergey Peleshanko,<sup>†</sup>  
Sergei Markutsya,<sup>†</sup> Myongsoo Lee,<sup>\*,‡</sup> and Yong-Sik Yoo<sup>‡</sup>

Department of Materials Science & Engineering, Iowa State University, Ames, Iowa 50011,  
and Department of Chemistry, Yonsei University, Seoul 120-749, Korea

Received March 18, 2002. In Final Form: September 6, 2002

Rod–coil molecules of 4,4'-bis[4-methyloxypoly(propyleneoxy)-propyloxy-4'-biphenyloxymethyl]biphenyl with 3, 6, 17, and 22 repeating propylene oxide units (**CRC-N**) have been investigated for their ability to form organized monolayers on a solid surface. We observed a complete spectrum of molecular reorganizations at variable surface pressure for the **CRC-17** molecule. These reversible molecular reorganizations, ranging from separated circular micelles composed of 20–30 molecules to a rectangular lattice of circular micelles with the unit cell of 10.6 × 9.7 nm and further to a perfectly ordered lamellar structure with 6.5 nm periodicity, all are induced by the variation of surface area available for the molecule. We suggest that continuous compression results in folding of water-soluble flexible tails and their desorption from the air–water interface into the water subphase. As a result, the effective content of the rod blocks at the air–water interface is changing continuously from 20% for close to zero surface pressure to 50% in the wake of monolayer collapse, initiating molecular reorganizations predicted by the theoretical models. Variable “effective” composition at the air–water interface for constant chemical composition provides an efficient mechanism for initiation of structural reorganizations within the monolayer.

## 1. Introduction

Rod–coil molecules have been introduced as a novel type of block copolymers with unique microstructural organization combining both liquid-crystalline (LC) and microphase-separated structures.<sup>1,2</sup> These molecules are capable of self-assembling in a variety of nanostructures in the bulk state and in solution. Lamellar, zigzag, cylindrical, and various micellar morphologies were predicted and found for rod–coil molecules with variable chemical composition.<sup>3–8</sup> The possibility of the formation of this type of ordered structures within a monomolecular layer of amphiphilic rod–coil molecules on a solid substrate is not verified to date. The presence of the solid substrate induces additional spatial constraints on molecular packing that can affect resulting morphologies. On the other hand, the variation of surface pressure may lead to variable molecular ordering even if the chemical composition remains unchanged. For amphiphilic rod–coil molecules, water-soluble flexible tails can submerge in a water subphase during compression, thus forming a thin polymer layer enriched with water molecules beneath the rod blocks and changing the effective composition at the air–water interface.<sup>9,10</sup> The ability of surface active rod–coil molecules with water-soluble blocks to adsorb on solid surfaces

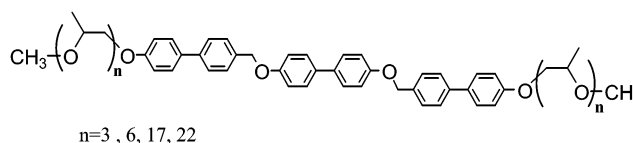


**Figure 1.** Chemical formula of the rod–coil molecules **CRC-N**.

and form adsorbed layers with organized surface nanostructures is an intriguing question relevant to a wide variety of prospective applications in surface and colloidal sciences such as multifunctional adaptive surfaces responsive to variation of external physical or chemical stimuli.

In this paper, we report direct observation of multiple molecular reorganizations for Langmuir monolayers from amphiphilic rod–coil molecules with poly(propylene oxide) (PPO) flexible tails of variable length. As has been recently demonstrated, these molecules with different chemical composition form a variety of LC structures of cubic, columnar, and hexagonal types in the bulk state.<sup>11,12</sup>

## 2. Experimental Section

Synthesis of all coil–rod–coil (CRC) molecules of 4,4'-bis[4-methyloxypoly(propyleneoxy)-propyloxy-4'-biphenyloxymethyl]biphenyl with variable length of the flexible tails of 3, 6, 17, and 22 propylene oxide units (**CRC-3**, **CRC-6**, **CRC-17**, and **CRC-22**) has been recently described (Figure 1).<sup>12</sup> The substrates were polished silicon wafers (Semiconductor Processing Co.) of the {100} orientation. Wafers were treated in “piranha” solution (30% hydrogen peroxide/94% sulfuric acid, 1:3 ratio) according to the standard procedure described elsewhere.<sup>13</sup> Monomolecular films

\* To whom correspondence should be addressed. E-mail: vladimir@iastate.edu (V. V. Tsukruk); mslee@yonsei.ac.kr (M. Lee).

<sup>†</sup> Iowa State University.

<sup>‡</sup> Yonsei University.

(1) Klok, A. H.; Lecommandoux, S. *Adv. Mater.* **2001**, *13*, 1217.  
Brunsveld, L.; Folmer, B. J.; Meijer, E. W.; Sijbesma, R. P. *Chem. Rev.* **2001**, *101*, 4071.

(2) Stupp, S. I. *Curr. Opin. Colloid Interface Sci.* **1998**, *3*, 20.

(3) Semenov, A. N.; Vasilenko, S. V. *Sov. Phys. JETP* **1986**, *63*, 70.  
Williams, D. R.; Fredrickson, G. H. *Macromolecules* **1992**, *25*, 3561.

(4) Li, W.; Gersappe, D. *Macromolecules* **2001**, *34*, 6783.

(5) Tew, G. N.; Pralle, M. U.; Stupp, S. I. *J. Am. Chem. Soc.* **1999**, *121*, 9852. Stupp, S. I.; LeBonheur, V.; Walker, K.; Li, L. S.; Huggins, K. E.; Kesser, M.; Amstutz, A. *Science* **1997**, *276*, 384.

(6) Chen, J. T.; Thomas, E. L.; Ober, C. K.; Mao, C. P. *Science* **1996**, *273*, 384.

(7) Lee, M.; Cho, B. K.; Zin, W. C. *Chem. Rev.* **2001**, *101*, 3869.

(8) Zubarev, E. R.; Pralle, M. U.; Li, L.; Stupp, S. I. *Science* **1999**, *283*, 523.

(9) Kampf, J. P.; Frank, C. W.; Malmstrom, E. E.; Hawker, C. J. *Langmuir* **1999**, *15*, 227.

(10) Xu, Z.; Holland, N. B.; Marchant, R. E. *Langmuir* **2001**, *17*, 377.

(11) Cho, B. K.; Lee, M.; Oh, N.; Zin, W. C. *J. Am. Chem. Soc.* **2001**, *123*, 9677. Lee, M.; Cho, B. K.; Oh, N.; Zin, W. C. *Macromolecules* **2001**, *34*, 1987. Lee, M.; Kim, J. W.; Hwang, I. W.; Kim, Y. R.; Oh, N.; Zin, W. C. *Adv. Mater.* **2001**, *13*, 1363.

(12) Lee, M.; Cho, B. K.; Jang, Y. G.; Zin, W. C. *J. Am. Chem. Soc.* **2000**, *122*, 7449.

(13) Tsukruk, V. V.; Bliznyuk, V. N. *Langmuir* **1998**, *14*, 446.

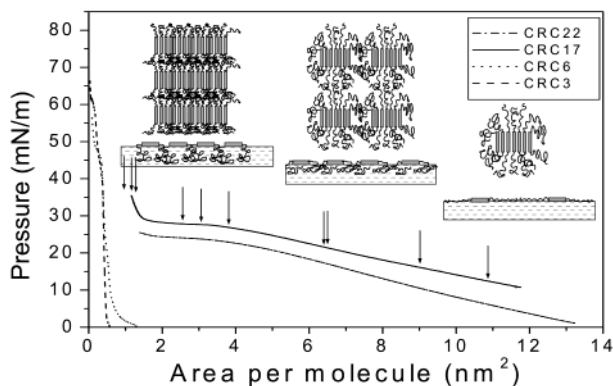


**Figure 2.** Pressure–area isotherms for rod–coil molecules. For the **CRC-17** molecule, arrows indicate various samples studied in detail and inserts show different molecular structures for the monolayer at different pressures, from right to left: circular micelles, rectangular lattice of circular micelles, and lamellar ordering of coalesced micelles. Schematics show both side view and top view for each molecular ordering of **CRC-17**.

of the dendritic compounds were prepared by the Langmuir technique on an RK-1 trough (Riegel & Kirstein, GmbH). The compounds were dissolved in chloroform (Fisher, reagent grade) to concentrations of 0.10–0.50 mmol/L. The solution was spread over the water (NanoPure, >18 M $\Omega$  cm) subphase. Monomolecular films of the compounds were deposited on silicon substrates according to the standard procedure.<sup>14</sup> The monolayer was allowed to dry for 30 min and then compressed at 100  $\mu$ m/s until the desired surface pressure and deposited onto a hydrophilic surface at a lift speed of 50  $\mu$ m/s.

Ellipsometric measurements of the monolayer thickness were carried out with a COMPEL automatic ellipsometer (InOmTech, Inc.). Atomic force microscopy (AFM) studies were performed with Dimension-3000 and Multimode microscopes (Digital Instruments) in the tapping mode according to an experimental procedure described in detail earlier.<sup>15,16</sup> The geometrical parameters of all molecules were estimated from the molecular models built with the Cerius<sup>2</sup> program.

### 3. Results

Figure 2 shows representative  $\pi$ – $A$  isotherms for **CRC-N** samples. The isotherms for **CRC-3** and **CRC-6** display the surface pressure increasing sharply before the monolayer collapse. The surface area per molecule at collapse increases with increasing length of the flexible tails. The  $\pi$ – $A$  isotherm for **CRC-3** shows an increase in the surface pressure near 0.5 nm<sup>2</sup> per molecule, while the **CRC-6** isotherm shows a slightly larger area, 0.74 nm<sup>2</sup> per molecule. The complete pressure–area isotherm for the molecule with the longest tails, **CRC-22**, was technically difficult to obtain within one run due to high cross-sectional area and limited compression ratio of the LB trough. A major part of the isotherm for **CRC-22** is similar to that for **CRC-17** discussed below (Figure 2).

The surface area occupied by the hydrophobic rod block (3.1 nm long) was calculated to be about 1.5 nm<sup>2</sup> when the flat molecule is on the surface and decreases to 0.3 nm<sup>2</sup> if the molecule is oriented along the surface normal. Therefore, we can conclude that rod–coil molecules with 3 and 6 PPO units do not show stable amphiphilic behavior and detectable surface pressure rise is attributed only to the monolayer collapse. Obviously, very short hydrophilic tails do not provide amphiphilic balance sufficient to form a stable monolayer. AFM observations demonstrate

uneven surface morphology with surface domain and wrinkles associated with the collapsed state.

Unlike the shorter tailed molecules, the **CRC-17** molecules with longer flexible tails demonstrated classic amphiphilic behavior with steadily rising surface pressure for the surface area per molecule below 13 nm<sup>2</sup>, constant pressure for the surface area within 3.3–1.5 nm<sup>2</sup>, and final collapse for the surface area below 1 nm<sup>2</sup> (Figure 2). Reversibility of the monolayer behavior at the air–water interface was tested by repeating compression–expansion cycles for the monolayer several times. A very modest hysteresis was observed for each cycle for **CRC-17** (as well as for **CRC-22**), indicating modest creep and a short recovery time for the long PPO chains to expand to the original random coil conformation. The **CRC-17** monolayers were deposited on the solid substrates at different surface pressures, from different solutions, and under variable “annealing” conditions (monolayer relaxation before the deposition) and showed consistent results. The **CRC-17** monolayer possesses a variety of molecular organizations at various surface pressures resembling that predicted for the bulk rod–coil molecules.<sup>3,4</sup>

AFM observations showed that monolayer films were smooth and uniform on a microscopic scale (5–20  $\mu$ m across). Higher magnification revealed a variety of surface morphologies (Figures 3 and 4). At a high surface area of 7–12 nm<sup>2</sup> close to the cross-sectional area of the **CRC-17** molecule lying flatly on a surface (about 8 nm<sup>2</sup>), a grainy surface morphology was visible with a distance between the grains of 12  $\pm$  4 nm and a lateral dimension of the grains of 12  $\pm$  3 nm (evaluated taking into account the tip radius of 20 nm) that is close to the length of the molecules in the nearly extended conformation (12–16 nm, depending upon the degree of PPO chain curling). Short-range ordering in the micellar packing was expanded over 5–7 grains as demonstrated by cross sections (Figure 3). Heights of these grains were in the range of 0.3–0.4 nm that corresponded to the overall thickness of the monolayer of 0.34 nm obtained from ellipsometry. This confirmed a flat arrangement of **CRC-17** molecules under these conditions.

Compression of the **CRC-17** monolayer to a surface area per molecule below 7 nm<sup>2</sup> led to the first signs of aggregation of grainy structures and the formation of poorly ordered clusters as confirmed by the appearance of a diffuse halo on 2D Fourier transforms (Figure 3B). Further compression below 4 nm<sup>2</sup> (significantly smaller than the molecular area of a flat molecule, 8 nm<sup>2</sup>) resulted in the formation of a relatively well-ordered lattice of rectangular type as confirmed by the four-point Fourier transform (Figure 4A). The unit cell dimensions are 10.6  $\times$  9.7 nm. The thickness of the monolayer in this state increased 2-fold to 0.6–0.75 nm.

Finally, at a lower surface area per molecule (below 2.5 nm<sup>2</sup>), on the verge of monolayer collapse (the molecular area of the rigid block is about 1.5 nm<sup>2</sup>), a perfect lamellar lattice becomes visible with periodicity of 6.5  $\pm$  0.6 nm (Figure 4B–D). The lamellae are very well-ordered on a microscopic scale and possess high orientational ordering as can be seen from the 2D Fourier pattern (Figure 4B). Uniform height is observed within the lamellae. Across the lamellar structures, 4–5 nm long elevations are separated by 2 nm long grooves of 0.3 nm depth. On a larger scale, micrometer size domains possess sharp boundaries of abrupt change of lamellar orientation and minor bending of the lamellae within the domains (Figure 4D). The thickness of the monolayer increases to 1.5 nm

(14) Tsukruk, V. V.; Bliznyuk, V. N.; Hazel, J.; Visser, D.; Everson, M. P. *Langmuir* **1996**, *12*, 4840.

(15) Tsukruk, V. V. *Rubber Chem. Technol.* **1997**, *70*, 430.

(16) Tsukruk, V. V.; Reneker, D. H. *Polymer* **1995**, *36*, 1791.

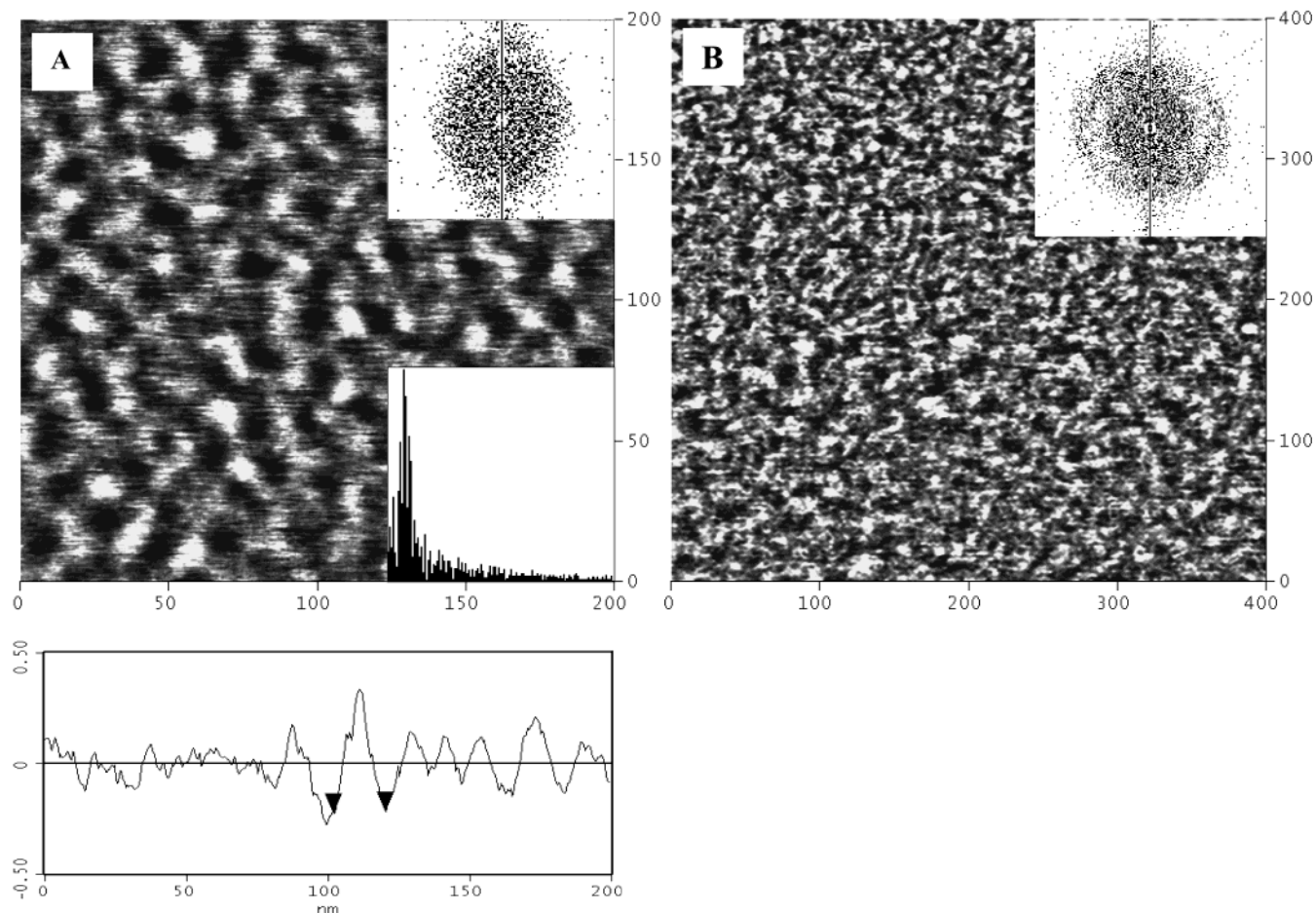


**Figure 3.** AFM images of the **CRC-17** monolayer at low surface pressures: (A) Surface cross section and topographical image at the surface area of  $7.7 \text{ nm}^2$  per molecule,  $200 \times 200 \text{ nm}$ ; the Z-range is  $0.8 \text{ nm}$ ; the inserts show the 2D Fourier transform of the image and the 1D Fourier transform of the surface cross section. (B) Phase image at the surface area of  $6 \text{ nm}^2$  per molecules,  $400 \times 400 \text{ nm}$ ; the Z-range is  $3^\circ$ ; the insert shows the 2D Fourier transform.

in this range and rises to  $4 \text{ nm}$  for surface areas below  $1.5 \text{ nm}^2$ , within the collapse region.

Molecular reorganization of the rod-coil molecules within the Langmuir monolayer can be understood considering theoretical treatment of phase states of rod-coil molecules in the bulk state and known behavior of water-soluble flexible chains at the air-water interface.<sup>3,4</sup> First, for a given chemical composition of **CRC-17** molecules with a volume fraction of the rod block of about 20% (as calculated from volume fractions of different blocks), theory predicts the formation of cylindrical micelles and their aggregates with rod blocks tightly packed and surrounded by coil blocks. The 2D analogue of a cylindrical micelle is a circular micelle. Ordered lattices of cylindrical structures are expected for a rod volume content higher than 30%. Finally, for a rod content higher than 50%, the formation of a lamellar morphology is expected. Although the phase transition theories discussed consider a diblock rod-coil molecule, we suggest that the same transitions and phases can be expected for a triblock rod-coil molecule. This is confirmed by numerous studies of bulk morphologies of block copolymers. For example, Molau<sup>17</sup> and Dawkins<sup>18</sup> suggested similar models for expected morphology AB and ABA block copolymers with varying volume fractions.

(17) Molau, G. E. In *Block Copolymers*; Aggarwal, S. L., Ed.; Plenum: New York, 1970.

(18) Dawkins, J. V. In *Block Copolymers*; Allport, D. C., James, W. H., Eds.; John Wiley & Sons: New York, 1973.

Indeed, we observed that at a very low surface pressure where molecules lie flat and the molecular area is close to unperturbed molecular dimensions, the rod-coil molecule forms micellar structures with dimensions close to the length of the molecule with slightly coiled tails. Taking a molecular area of about  $8 \text{ nm}^2$  and a packing coefficient of 70%, we can estimate that a single aggregate contains 20–30 molecules packed in a manner similar to a “monolayer” puck proposed by Fredrickson for the bulk structure (Figure 2).<sup>3</sup>

Decreasing the surface area available for the rod-coil molecule results in both significant shrinkage of intermicellar distance and increasing layer thickness. This kind of transition can be associated with molecular reorganization caused by partial desorption of water-soluble tails from the air-water interface into the aqueous phase.<sup>10</sup> At higher surface pressures, the enthalpy gain achieved by this reorganization exceeds the loss of entropy caused by folded and compressed flexible tails. This restructuring leads to the formation of an ordered lattice from micelles composed of the topmost rod block and partially submerged flexible tails (Figure 2). The total layer thickness doubles and the “effective” content of the rod blocks in the topmost layer increases to 31% due to partial submerging of the flexible tails. This composition at the air-water interface should favor cylindrical packing of micellar aggregates.<sup>4</sup> Indeed, this type of molecular reorganization is observed for the **CRC-17** monolayer at this surface pressure. The total number of molecules in one circular micelle estimated

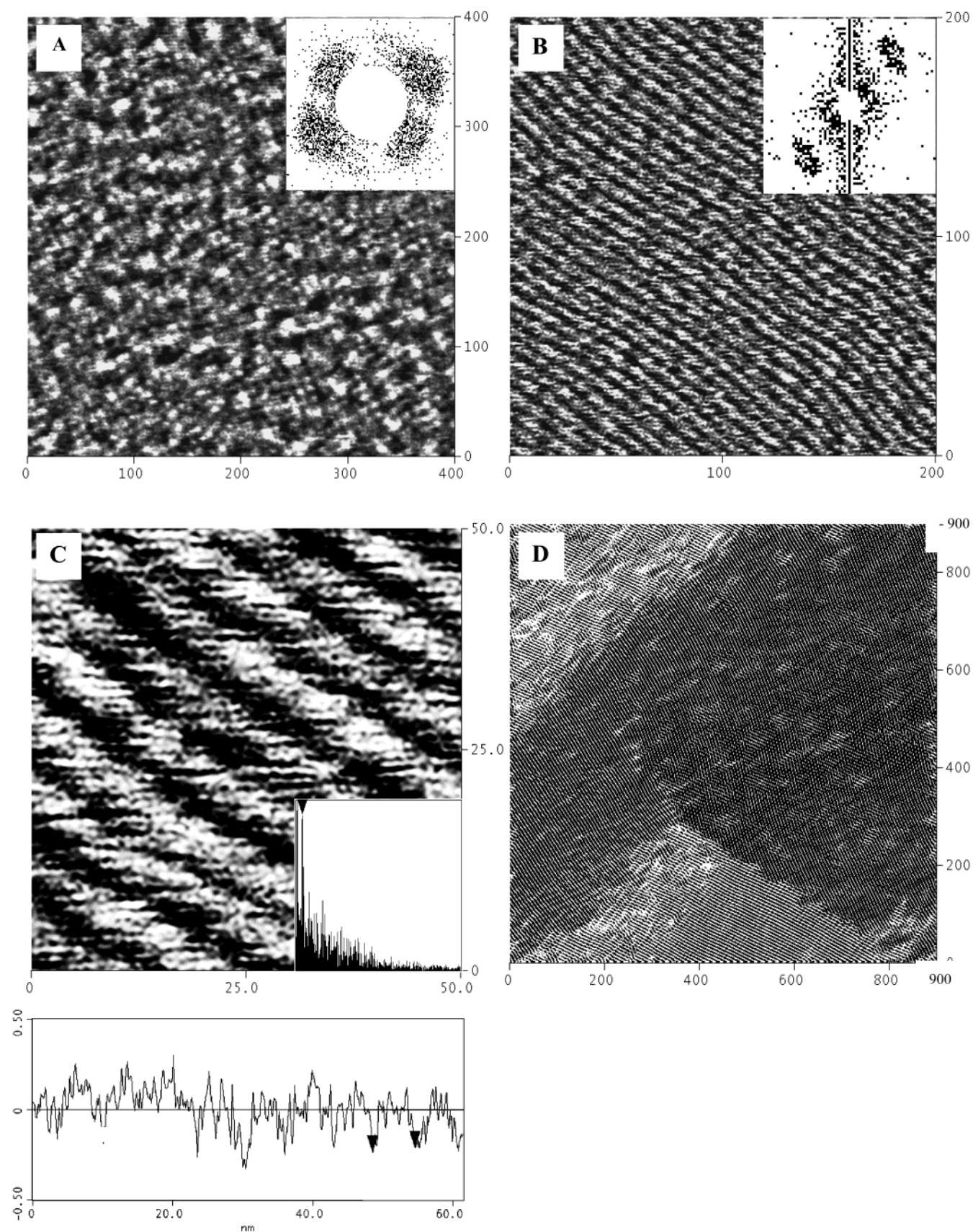


**Figure 4.** AFM images of the **CRC-17** monolayer at high surface pressures: (A) Topographical image at the surface area of 3.6 nm<sup>2</sup> per molecule, 400 × 400 nm; the Z-range is 1 nm; the insert shows the 2D Fourier transform. (B) Topographical image at 2.2 nm<sup>2</sup> per molecule, 200 × 200 nm; the Z-range is 0.8 nm; the insert shows the 2D Fourier transform. (C) Higher resolution topographical image at the surface area of 2.2 nm<sup>2</sup> per molecule and surface cross section, 50 × 50 nm; the Z-range is 1 nm; the insert shows the 1D Fourier transform of the surface cross section. (D) Topographical image at the monolayer with lamellar domains, 900 × 900 nm; the Z-range is 1 nm; domain boundaries with abrupt changes of lamellar structure are visualized by illumination.

from the unit cell dimensions remains unchanged (20–30 molecules). The rectangular unit cell observed is different from the hexagonal structure predicted for the bulk state.<sup>4</sup> However, it is similar to the tetragonal lattice of micellar aggregates with unit cell parameters of  $9.0 \times 8.3$  nm observed for this molecule in the bulk LC state.<sup>9</sup>

The compression of the monolayer to the surface area comparable with rod-block dimensions initiates a second molecular reorganization. This reorganization can be related to the folding of the flexible tails and their dehydration due to expelling associated water molecules from densely packed areas beneath the air–water interface (Figure 2).<sup>10</sup> In this state, flexible tails can adopt a brushlike conformation increasing the total thickness of the layer to about 1.5 nm. The thickness of grafted flexible molecules of comparable molecular weight is within 1–3 nm depending upon the grafting density.<sup>19–21</sup> As a result of chain desorption, the effective content of the rod blocks at the air–water interface increases further to about 50%, thus causing the formation of lamellar structures favorable for such content.<sup>4</sup> Micelles are coalesced to form uniform lamellae. Further compression leads to the monolayer collapse and the formation of the second layer.

**CRC-22** molecules with a lower content of rod blocks (below 15%) do not show the richness of the phase behavior of the previous molecule despite a similar shape of the pressure–area isotherm (Figure 2). This was puzzling considering that even modest compression would result in sufficient change of effective composition and, thus, similar molecular reorganizations. We suggest that a very high fraction of water-soluble blocks disturbs a delicate amphiphilic balance of the rod–coil molecules at the air–water interface, preventing reorganization of rod blocks immersed with a sea of hydrophilic block beneath. Probably, steric constraints imposed by a high volume of PPO blocks compressed in the water subphase on chemically attached rod blocks affect their ability to aggregate in ordered structures.

In fact, the monolayer displays poorly ordered micellar aggregates at all pressures. Only at the highest reachable pressure, in the collapse region (area per molecule of below  $1.5 \text{ nm}^2$ ), weak tracks of lamellar structures within the collapsed monolayer have been observed. The thickness of the monolayer increases from 0.6 nm at  $10 \text{ nm}^2$  per

molecule to 4.1 nm at  $1.5 \text{ nm}^2$  per molecule at the highest pressure. The thickness of the monolayer at higher surface pressures indicates a rearrangement of the coil blocks, but the lamellar structure formed is incomplete. We suggest that unlike the **CRC-17** molecules, which partially submerged the PPO coils, the **CRC-22** molecules fully submerge under higher pressure creating a bilayer of compressed molecules. Instead of submerging the tails until the volume fraction is favorable to a phase change, the entire molecule is pushed out of the surface plane and supports the molecules that remain at the air/water interface, thereby increasing the monolayer thickness while having little noticeable effect on the surface morphology.

#### 4. Conclusions

In conclusion, we observed a complete spectrum of molecular reorganizations predicted by the theoretical model for the rod–coil molecule with variable content of rod blocks. Amphiphilic rod–coil molecules with water-soluble flexible tails formed ordered monolayers at the air–water interface. We observed coalescence of individual circular micelles of 12 nm across to a rectangular lattice of circular micelles of  $10.6 \times 9.7$  nm and further to a perfectly ordered lamellar structure with 6.5 nm periodicity, all induced by the variation of the surface area available for rod blocks at the air–water interface. Continuous compression results in folding of water-soluble flexible tails and their desorption from the air–water interface into the water subphase, followed by their compaction and expulsion of water. As a result, the effective content of the rod blocks at the air–water interface is changing continuously from 20% to 50%, initiating molecular reorganizations predicted by the theoretical model. Variable effective composition at the air–water interface for constant chemical composition provides an efficient mechanism for initiation of structural reorganizations within the monolayer. These transformations occur at effective volume compositions close to the ones predicted for the bulk state despite constraints imposed by the solid substrate.

**Acknowledgment.** Funding from the National Science Foundation, DMR-0074241, Grant M01-C03 from Department of Commerce through National Textile Center, and support from CRM-KOSEF(2001) and KRF(BSRI DP0228) are gratefully acknowledged. We thank A. Greco for technical assistance with experiments.

(19) Karim, A.; Tsukruk, V. V.; Douglas, J. F.; Satija, S. K.; Fetters, L. J.; Reneker, D. H.; Foster, M. D. *J. Phys. II* **1995**, *5*, 1441.

(20) Luzinov, I.; Julthongpipit, D.; Malz, H.; Pionteck, J.; Tsukruk, V. V. *Macromolecules* **2000**, *33*, 1043.

(21) Halperin, A.; Tirrell, M.; Lodge, T. P. *Adv. Polym. Sci.* **1992**, *100*, 33.